



# Macrodasines A–G, macroline indole alkaloids incorporating fused spirocyclic tetrahydrofuran–tetrahydrofuran and tetrahydrofuran–tetrahydropyran rings

Shin-Jowl Tan<sup>a</sup>, Ward T. Robinson<sup>a</sup>, Kanki Komiyama<sup>b</sup>, Toh-Seok Kam<sup>a,\*</sup>

<sup>a</sup> Department of Chemistry, University of Malaya, 50603 Kuala Lumpur, Malaysia

<sup>b</sup> Center for Basic Research, Kitasato University, 5-9-1, Shirokane, Minato-ku, Tokyo 108-8642, Japan

## ARTICLE INFO

### Article history:

Received 14 January 2011

Received in revised form 8 March 2011

Accepted 28 March 2011

Available online 2 April 2011

### Keywords:

Spirocyclic alkaloids

NMR

X-ray

*Alstonia*

## ABSTRACT

The bark extract of the Malayan *Alstonia angustifolia* Wall provided the spirocyclic alkaloids macrodasines A–G. The structures of the new compounds were established by analysis of the spectroscopic data and in the case of macrodasines A and B confirmed by X-ray diffraction analysis. Macrodasines A, B, C, and G incorporate fused spirocyclic tetrahydrofuran–tetrahydrofuran rings, while macrodasines D, E, and F incorporate fused tetrahydrofuran–tetrahydropyran rings. Macrodasines B, C, and E were found to show moderate levels of activity in reversing multidrug-resistance in drug-resistant KB cells.

© 2011 Elsevier Ltd. All rights reserved.

## 1. Introduction

Plants of the genus *Alstonia*<sup>1</sup> (Apocynaceae) are fertile sources of structurally novel as well as biologically active alkaloids.<sup>2–33</sup> The *Alstonia* bisindoles in particular are known for displaying significant in vitro antiamoebic activity against *Plasmodium falciparum* (the causative agent of Malaria), as well as cytotoxic activity against several human cancer cell lines.<sup>4–10</sup> Other bioactive alkaloids from *Alstonia* include the indole alkaloid, actinophyllin acid from the Australian *Alstonia actinophylla*, which was reported to be an effective inhibitor of carboxypeptidase U (CPU),<sup>11</sup> and the strychnan alkaloids, alstolucines A, B, and F, from the Malayan *Alstonia spatulata*, which reverse multidrug-resistance in drug-resistant KB cells.<sup>12</sup> We recently reported the structure of the novel *Alstonia* alkaloid, bipleiophyllin, a cytotoxic bisindole constituted from the bridging of two indole moieties by an aromatic spacer unit,<sup>5</sup> as well as several unusual indole alkaloid-pyrrole, -pyrone, and -carbamic acid adducts from the stem-bark extract of *A. angustifolia* Wall.<sup>13</sup> In continuation of our studies of biologically active alkaloids from Malaysian *Alstonia*,<sup>5,12–20</sup> we wish to report the structures of the novel spirocyclic alkaloids, macrodasines A–G, isolated from the stem-bark extract of the same plant.

## 2. Results and discussion

We previously reported the isolation and structure elucidation of macrodasine A (**1**), which was isolated in minute amounts from the bark extract of *Alstonia macrophylla*.<sup>14,18</sup> The structure of **1** was established based on interpretation of the NMR and MS data, which revealed a macroline indole alkaloid incorporating a 1,6-dioxaspiro [4,4]nonane unit fused onto the macroline residue. An alternative structure incorporating contiguously fused tetrahydropyran and tetrahydrofuran rings attached to the same macroline residue was ruled out by the observation that acetylation with acetic anhydride/pyridine gave a diacetylated derivative, **8**. The relative configurations at the various stereogenic centers were established by the application of extensive NOE experiments. Since we have now isolated more macrodasine A (**1**) from *A. angustifolia*, we were therefore able to carry out a more detailed stereochemical study.

In general the NMR data for all seven alkaloids indicated that the configurations of the stereogenic centers in the macroline portion of the molecule are similar to those of a macroline indole alkaloid. In addition, the EI/MS showed mass fragments at *m/z* 197, 182, 181, 170, and 144, which are typical of macroline derivatives.<sup>34</sup> The observed NOEs between 18-methyl and H-17 $\alpha$  as well as H-20, fixed the E/F ring junction stereochemistry as *cis* (18-Me and H-20 both  $\alpha$ ). The resonance for H-20 was observed as a doublet of doublets with *J* 12 and 8 Hz. Decoupling experiments indicated that the splittings were due to coupling with the two C-21 hydrogens. Since the stereochemistry of H-20 has been fixed as  $\alpha$ , the 12 Hz coupling must be due to coupling to

\* Corresponding author. Tel.: +60 3 79674266; fax: +60 3 79674193; e-mail address: [tskam@um.edu.my](mailto:tskam@um.edu.my) (T.-S. Kam).

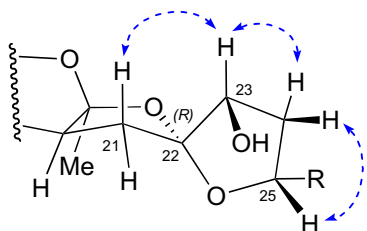
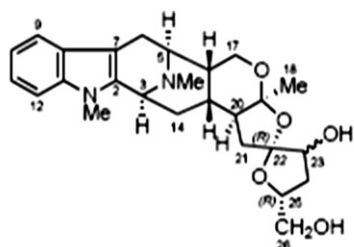
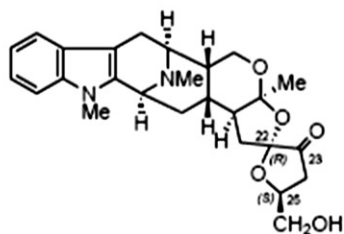


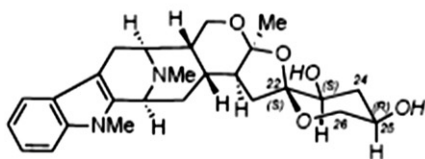
Fig. 1. Selected NOEs of **1** (R=CH<sub>2</sub>OH).



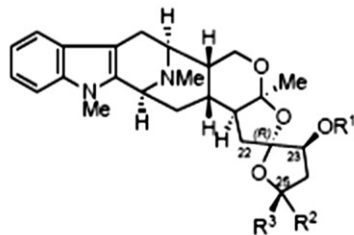
Macrodasine A (**1**)  
23-βOH (23S) (revised)  
23-αOH (23R) (previous assignment)



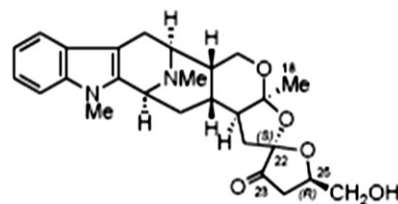
**3**



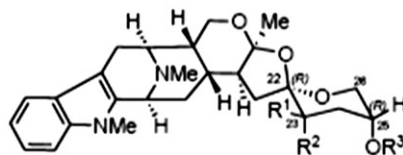
**6**



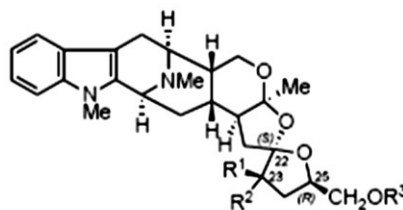
**8** R<sup>1</sup> = Ac, R<sup>2</sup> = CH<sub>2</sub>OAc, R<sup>3</sup> = H (23S, 25R)  
**11** R<sup>1</sup> = H, R<sup>2</sup> = H, R<sup>3</sup> = CH<sub>2</sub>OH (23S, 25S)



**2**



**4** R<sup>1</sup> = OH, R<sup>2</sup> = H, R<sup>3</sup> = H (23R)  
**5** R<sup>1</sup> = H, R<sup>2</sup> = OH, R<sup>3</sup> = H (23S)  
**12** R<sup>1</sup> = OAc, R<sup>2</sup> = H, R<sup>3</sup> = Ac (23R)



**7** R<sup>1</sup> = H, R<sup>2</sup> = OH, R<sup>3</sup> = H (23S)  
**9** R<sup>1</sup> = OH, R<sup>2</sup> = H, R<sup>3</sup> = H (23R)  
**10** R<sup>1</sup> = H, R<sup>2</sup> = OAc, R<sup>3</sup> = Ac (23S)

as a result, both the α and β hydrogens at C-21 could not be distinguished. In the previous report, it was noted that conversion of **1** to the diacetate derivative **8** resulted in the removal of the H-21/H-24 overlap to some extent.<sup>18</sup> In the present study, it was found that a further improvement in the spectrum could be achieved by the use of CD<sub>2</sub>Cl<sub>2</sub> in place of CDCl<sub>3</sub>, which in the case of **1** resulted in an improved separation of the key signals, viz., H-21β (δ 2.36, t, J=12 Hz) and H-24β (δ 1.80, dd, J=13.4, 7 Hz). By the use of these methods, meaningful NOEs could now be obtained (Fig. 1). Thus, irradiation of H-23 caused NOE enhancement of H-21β and vice versa, which allowed the assignment of the configuration at the spirocarbon at C-22 as R.

H-21β. Examination of the structure of **1**, showed that the NOE interaction between H-21 and H-23 is of crucial importance in the assignment of the configuration at the spirocyclic center at C-22 (Fig. 1). The <sup>1</sup>H NMR spectrum (Table 1) of **1** was however complicated by the overlap of some key signals, such as, for example, H-21/H-24. As

Examination of models showed that the configuration of the hydroxy-substituted C-23 could not be established based solely on NOE experiments due to the fact that H-21β would experience NOE interaction with H-23 regardless of whether H-23 is α- or β-oriented. However, had H-23 been β, it would be expected (based on

**Table 1**  
<sup>1</sup>H (400 MHz) NMR data of **1**–**3**, **7**, and **9**–**11**

Position	<b>1</b> <sup>a</sup>	<b>1</b> <sup>b</sup>	<b>2</b> <sup>a</sup>	<b>3</b> <sup>a</sup>	<b>7</b> <sup>a</sup>	<b>9</b> <sup>a</sup>	<b>10</b> <sup>a</sup>	<b>11</b> <sup>a</sup>
3	3.95 (t, 3)	4.00 (m)	3.94 (t, 3)	3.96 (m)	3.95 (m)	4.02 (m)	3.93 (m)	3.96 (m)
5	2.98 (d, 7)	3.00 (d, 7)	2.99 (d, 7)	2.98 (d, 7)	3.50 (d, 7)	3.04 (d, 7)	2.98 (d, 7)	2.98 (d, 7)
6β	2.39 (m)	2.45 (m)	2.41 (d, 17)	2.44 (d, 17)	2.42 (d, 17)	2.42 (d, 17)	2.40 (d, 17)	2.42 (d, 17)
6α	3.27 (dd, 17, 7)	3.25 (dd, 17, 7)	3.28 (dd, 17, 7)	3.26 (dd, 17, 7)	3.27 (dd, 17, 7)	3.28 (dd, 17, 7)	3.26 (dd, 17, 7)	3.27 (dd, 17, 7)
9	7.50 (br d, 8)	7.45 (d, 7.8)	7.50 (br d, 8)	7.51 (d, 8)	7.50 (d, 8)	7.50 (d, 8)	7.50 (d, 8)	7.51 (d, 8)
10	7.12 (br t, 8)	7.05 (t, 7.8)	7.12 (td, 8, 1)	7.12 (td, 8, 1)	7.12 (t, 8)	7.12 (t, 8)	7.11 (t, 8)	7.13 (td, 8, 1)
11	7.21 (td, 8, 1)	7.15 (t, 7.8)	7.21 (td, 8, 1)	7.21 (td, 8, 1)	7.21 (t, 8)	7.21 (t, 8)	7.20 (t, 8)	7.22 (td, 8, 1)
12	7.31 (br d, 8)	7.31 (d, 7.8)	7.31 (br d, 8)	7.31 (d, 8)	7.30 (d, 8)	7.31 (d, 8)	7.30 (d, 8)	7.32 (d, 8)
14β	1.55 (ddd, 13, 5, 3)	1.57 (m)	1.56 (m)	1.53 (ddd, 13, 5, 2)	1.52 (ddd, 13, 5, 3)	1.53 (ddd, 13, 5, 3)	1.52 (m)	1.54 (ddd, 13, 4, 2)
14α	2.39 (m)	2.45 (m)	2.42 (m)	2.40 (td, 13, 5)	2.42 (m)	2.43 (td, 13, 5)	2.39 (m)	2.42 (m)
15	1.85 (m)	1.80 (m)	1.84 (dt, 12, 5)	1.83 (dt, 13, 5)	1.81 (m)	1.83 (dt, 13, 5)	1.77 (m)	1.85 (m)
16	2.03 (dt, 12, 5)	2.05 (m)	2.14 (m)	2.14 (dt, 11, 5)	2.16 (dt, 12, 5)	2.20 (dt, 12, 5)	2.15 (dt, 12, 5)	2.08 (dt, 12, 5)
17β	3.70 (dd, 12, 5)	3.65 (ddd, 12, 5, 1)	3.85 (dd, 12, 5)	3.85 (dd, 12, 5)	3.87 (dd, 12, 5)	3.83 (dd, 12, 5)	3.81 (dd, 12, 5)	3.73 (dd, 12, 5)
17α	4.04 (t, 12)	4.03 (m)	4.08 (t, 12)	3.98 (dd, 12, 11)	4.09 (t, 12)	4.12 (t, 12)	4.05 (t, 12)	4.07 (t, 12)
18	1.59 (s)	1.54 (s)	1.54 (s)	1.62 (s)	1.59 (s)	1.50 (s)	1.51 (s)	1.64 (s)
20	2.01 (dd, 12, 8)	1.98 (dd, 12, 8)	2.02 (m)	2.07 (dd, 12, 8)	1.85 (dd, 12, 8)	1.76 (dd, 12, 8)	1.75 (dd, 12, 8)	2.01 (dd, 12, 8)
21	1.85 (m) (α)	1.77 (dd, 12, 8) (α)	2.02 (m) (α)	1.75 (dd, 13, 8) (α)	2.00 (dd, 13, 8) (α)	2.09 (dd, 13, 12) (β)	2.00 (dd, 13, 8) (α)	1.87 (dd, 13, 8) (α)
21	2.39 (m) (β)	2.36 (t, 12) (β)	2.15 (dd, 13, 11) (β)	2.42 (dd, 13, 12) (β)	2.32 (t, 13) (β)	2.43 (dd, 13, 8) (α)	2.32 (t, 13) (β)	2.29 (t, 13) (β)
23	4.13 (d, 5) (α)	4.06 (d, 5)	—	—	3.95 (m) (β)	3.69 (d, 5) (α)	4.95 (dd, 7, 6)	3.96 (m) (α)
24	1.85 (m)	1.80 (dd, 13.4, 7) (β)	2.50 (dd, 17, 7)	2.53 (dd, 19, 8)	1.87 (m) (α)	1.78 (dd, 14, 2.4) (β)	2.05 (m)	1.93 (ddd,
12, 10.5, 9.5)								
24	2.39 (m)	2.39 (ddd, 13.4, 8.5, 5) (α)	2.52 (dd, 17, 8)	2.76 (dd, 19, 4)	2.08 (ddd, 13, 8, 5) (β)	2.56 (ddd, 14, 10, 5) (α)	2.05 (m)	2.17 (dt, 12, 8)
25	4.42 (m)	4.36 (m)	4.56 (m)	4.49 (dtd, 8, 4, 2)	4.32 (m)	4.37 (m)	4.47 (tt, 7, 5)	4.16 (m)
26	3.43 (dd, 12, 3)	3.36 (d, 12)	3.61 (dd, 12, 4)	3.55 (dd, 12, 4)	3.43 (dd, 12, 4)	3.45 (dd, 12, 1)	4.03 (dd, 12, 5)	3.42 (dd, 11.7, 2)
26	3.77 (dd, 12, 2)	3.67 (dd, 12, 2.7)	3.96 (dd, 12, 3)	3.86 (dd, 12, 2)	3.69 (dd, 12, 3)	3.88 (dd, 12, 2)	4.16 (dd, 12, 5)	3.71 (dd, 11.7, 2)
N(1)-Me	3.63 (s)	3.61 (s)	3.63 (s)	3.63 (s)	3.62 (s)	3.63 (s)	3.63 (s)	3.63 (s)
N(4)-Me	2.33 (s)	2.35 (s)	2.34 (s)	2.36 (s)	2.35 (s)	2.39 (s)	2.34 (s)	2.34 (s)
23-OH	—	—	—	—	—	—	—	3.16 (br d, 8)
23-OAc	—	—	—	—	—	—	2.05 (s)	—
25-OAc	—	—	—	—	—	—	2.06 (s)	—

<sup>a</sup> Measured in CDCl<sub>3</sub>.

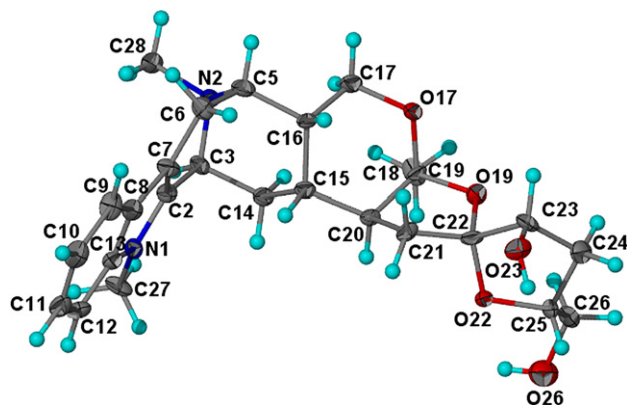
<sup>b</sup> Measured in CD<sub>2</sub>Cl<sub>2</sub>.

examination of models) to show NOE with both the H-21 (α and β), whereas if H-23 is α, it is expected to show NOE with H-21β only. Since NOE was observed with H-21β only, it might be inferred that the orientation of H-23 is α, although positive evidence for this conclusion is still required. Furthermore, the observed NOEs for H-23/H-24α and H-25/H-24β indicated that H-23 and H-25 have an *anti* relationship to each other, which in turn allowed the orientation of H-25 to be assigned as β (C-25R). The present assignments therefore indicated that while the previous assignment of the spirocenter configuration as 22R was correct, the previous assignment of the C-23 configuration as R required amendment to 23S in view of the present NOE data. As sufficient amounts of **1** were this time available, we were also able to attempt crystallization to obtain suitable crystals for X-ray diffraction. Macrodasine A (**1**) was found to crystallize from ethanol as colorless plates with mp 149–154 °C. Single-crystal X-ray diffraction analysis was carried, which confirmed the assignment of the configuration of the spirocyclic C-22 (based on NOE) as R. In addition, the X-ray data also confirmed the assignment of the configurations of the hydroxy-substituted C-23 and C-25, as 23S and 25R, respectively (Fig. 2).

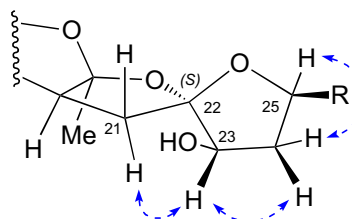
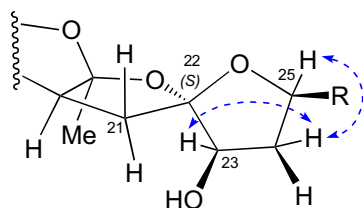
Macrodasine B (**2**) was also previously obtained from *A. macrophylla*.<sup>14</sup> It was isolated in even lesser amounts compared to **1** and as such, although the gross structure could be established, various stereochemical aspects remained to be determined with certainty. The present isolation of **2** in sufficient amounts from *A. angustifolia* has allowed the stereochemical aspects to be addressed in depth.

The MS and NMR data of **2** revealed the same basic skeleton as that of **1** with the macroline portion (rings A, B, C, D, and E) remaining essentially intact, but with changes occurring in rings F and G. The 2-D COSY spectrum showed, in addition to the NCHCH<sub>2</sub>, CHCH<sub>2</sub>, and NCHCH<sub>2</sub>CHCHCH<sub>2</sub>O fragments, which are common to **1**, a CH<sub>2</sub>CHCH<sub>2</sub>O fragment in place of the OCHCH<sub>2</sub>CHCH<sub>2</sub>O fragment observed in **1**. Examination of the <sup>13</sup>C NMR spectrum (Table 3) of **2** revealed that while the resonances of the two oxymethylenes at δ 64.8 and 63.1, corresponding to C-17 and C-26, and that of the oxymethine signal at δ 75.0 corresponding to C-25, as well as the quaternary carbon resonance due to the spiroacetal C-22 at δ 106.4, were intact, the other oxymethine at δ 77.7 corresponding to C-23 in **1** was absent in the spectrum of **2** and has been replaced by a ketone carbonyl resonance at δ 209.4. These features indicated that macrodasine B is the 23-oxo derivative of **1**, which was also consistent with the HMBC data. Paucity of material at the time of the previous report precluded further experiments required for establishment of the relative configurations of the stereogenic centers in the spiroketal portion of the molecule, which can now be addressed with sufficient amounts of **2** presently to hand from *A. angustifolia*.

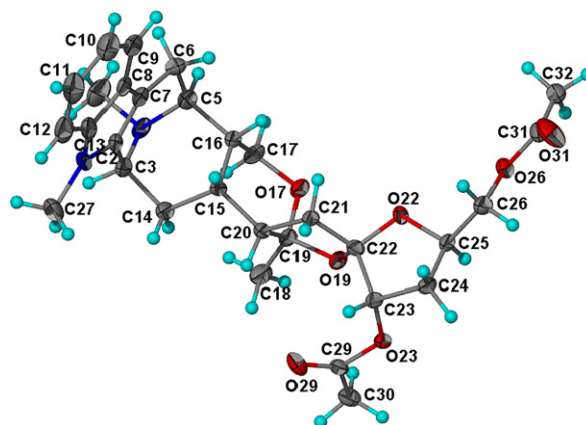
The NOE data showed that the ring junction stereochemistries for the C/D/E rings were similar to those of **1** and correspond to that of a typical macroline indole alkaloid. The stereochemistry of the E/F ring junction is also cis, as in **1**, from the observed 18-methyl/H-17α, H-20 NOEs. Determination of the configuration at the

Fig. 2. X-ray crystal structure of **1**.

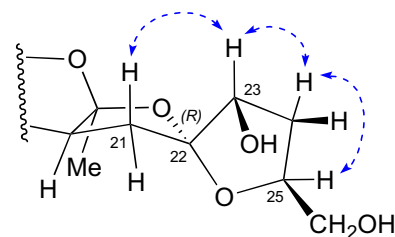
spirocyclic C-22 was in the present case not possible since C-23 is a ketone carbonyl in macrodasine B (**2**). Macrodasine B (**2**) was therefore first reduced by treatment with  $\text{NaBH}_4/\text{MeOH}$  to give a mixture of the epimeric alcohols, **7** and **9**, with the former obtained as the major epimer. Irradiation of H-23 of the major epimer **7**, resulted in NOE enhancement of H-21 $\alpha$  and vice versa (Fig. 3), which allowed the configuration of the spirocyclic C-22 as well as the stereogenic center at C-23 to be assigned as *S*. The reciprocal NOEs observed for H-23 $\beta$ /H-24 $\beta$  and H-25/H-24 $\alpha$  indicated that H-23 and H-25 are *anti* to each other, which in turn allowed the relative configuration of C-25 to be assigned as *R*. Irradiation of H-23 of the minor epimer **9**, on the other hand, did not have any effect on H-21 $\alpha$  as expected, but resulted instead in the enhancement of H-24 $\alpha$  (Fig. 4). Irradiation of H-24 $\alpha$  resulted in enhancement of H-25, which must therefore have  $\alpha$ -orientation (C-25*R*) as well (since H-23, H-24 $\alpha$ , H-25 are all *syn* to each other). These results are also consistent with those obtained from NOE experiments on the major epimer, which showed that the configuration of C-25 is *R*. Attempts to obtain crystals of **2** suitable for X-ray diffraction were not successful. However the diacetate derivative **10** derived from treatment of **7** with  $\text{Ac}_2\text{O}/\text{pyridine}$ , crystallized from EtOH as colorless needles, which on X-ray diffraction analysis (Fig. 5) provided confirmation of the stereochemical assignments of macrodasine B (**2**) described above based on NOE experiments on the epimeric alcohols **7** and **9**.

Fig. 3. Selected NOEs of **7** ( $\text{R}=\text{CH}_2\text{OH}$ ).Fig. 4. Selected NOEs of **9** ( $\text{R}=\text{CH}_2\text{OH}$ ).

Macrodasine C (**3**) was obtained as a light yellowish oil, with  $[\alpha]_{\text{D}}^{25} -45$  ( $c$  0.14,  $\text{CHCl}_3$ ). The IR spectrum showed absorptions due to OH ( $3467\text{ cm}^{-1}$ ) and five-membered cyclic ketone ( $1766\text{ cm}^{-1}$ )

Fig. 5. X-ray crystal structure of **10**.

functions, while the UV spectrum (228 and 286 nm) indicated the presence of an indole chromophore. The EIMS showed an  $\text{M}^+$  at  $m/z$  452, which indicated that **3** was isomeric with **2**. The  $^1\text{H}$  and  $^{13}\text{C}$  NMR data were also generally similar to those of macrodasine B (**2**) (Tables 1 and 3), except for differences in the shifts of C-18, C-20, C-22, and C-23. The 2-D NMR data of **3** were also similar to those of **2** indicating that **3** possesses the same carbon skeleton as **2**, with the tetrahydrofuran ring G incorporating a ketone functionality at C-23 and a secondary alcohol function at C-25. Macrodasine C (**3**) is therefore a stereoisomer of macrodasine B (**2**) and differs in the configuration of the spirocyclic center at C-22 and/or the stereo-center at C-25 in the tetrahydrofuran ring. As in the case of **2**, determination of the configuration of the spirocyclic C-22 required reduction of **3** to the alcohol derivative. In this instance only one product **11**, was obtained upon treatment of **3** with  $\text{NaBH}_4/\text{MeOH}$ . Irradiation of H-23 of **11** caused NOE enhancement of H-21 $\beta$  and vice versa only (Fig. 6), which allowed the configuration at C-22 in **11** (and **3**) to be determined as *R*. Based on arguments presented above in the case of **1**, it could also be inferred that since NOE was observed for H-21 $\beta$  only, on irradiation of H-23 (as opposed to both H-21 $\alpha$  and  $\beta$ ), the configuration of H-23 in **11** is  $\alpha$  or C-23*S*. The reciprocal NOEs observed for one of the C-24 hydrogens with H-23 and H-25, indicated that H-23 and H-25 are *syn* to each other. This in turn indicated that H-25 is  $\alpha$  (or C-25*S*). Unfortunately in this instance, X-ray confirmation could not be carried out due to lack of suitable crystals as well as paucity of material. In any case, while the assignment of the C-25 configuration is tentative, that of the spirocyclic center is firmly established.

Fig. 6. Selected NOEs of **11**.

Macrodasine D (**4**) was obtained as a light yellowish oil, with  $[\alpha]_{\text{D}}^{25} -12$  ( $c$  0.10,  $\text{CHCl}_3$ ). The UV spectrum was characteristic of an indole chromophore (229 and 286 nm), while the IR spectrum showed a broad band at  $3420\text{ cm}^{-1}$  indicating the presence of hydroxy functions. The EIMS of **4** showed a molecular ion at  $m/z$  454, which analyzed for  $\text{C}_{26}\text{H}_{34}\text{N}_2\text{O}_5$ , requiring 11 degrees of unsaturation (HREIMS found  $m/z$  454.2462, calcd for  $\text{C}_{26}\text{H}_{34}\text{N}_2\text{O}_5$ , 454.2468). As with macrodasine A (**1**), acetylation ( $\text{Ac}_2\text{O}/\text{pyridine}$ ) of **4** also

yielded a diacetate derivative **12** (EIMS  $m/z$  538,  $M^+$ ,  $C_{30}H_{38}N_2O_7$ ). The  $^{13}C$  NMR spectrum (Table 3) gave a total of 26 carbon resonances comprising three methyls, six methylenes, eleven methines, and six quaternary carbons in agreement with the molecular formula.

The NMR spectral data of **4** (Tables 2 and 3) showed a general similarity to those of macrodasine A (**1**) except for notable differences in the carbon shifts of C-22 to C-26 (Table 3) associated with the seventh ring, suggesting that the tetrahydrofuran ring G of **1** has been altered in **4**. However, the NMR data indicated that the fragments constituting the G ring remained the same, i.e., a methylene, two oxymethines, and one oxymethylene, in addition to the spirocarbon. This suggested a change in the structure involving the ring G portion of the molecule involving a different connectivity of the fragments. A possible structure is one where the fragments have been reconnected to furnish a six-membered ring G, in the form of a tetrahydropyranyl ring substituted by two hydroxyl groups, as shown in structure **4**. This was in fact suggested by the  $^{13}C$  shifts of the ring G carbons, which were shifted upfield (in particular the spirocenter C-22 at  $\delta$  106.6) compared with the corresponding shifts in **1** (Table 3), which is consistent with the presence of a spiro[4.5]decene moiety in **4**.<sup>35</sup>

**Table 2**  
 $^1H$  (400 MHz) NMR data of **4**–**6**, and **12**

Position	<b>4</b> <sup>a</sup>	<b>5</b> <sup>a</sup>	<b>5</b> <sup>b</sup>	<b>6</b> <sup>a</sup>	<b>6</b> <sup>c</sup>	<b>12</b> <sup>a</sup>
3	3.96 (m)	3.96 (m)	3.67 (m)	3.94 (m)	3.88 (m)	4.04 (m)
5	2.96 (d, 7)	2.98 (d, 7)	2.61 (d, 7)	2.97 (d, 7)	2.90 (d, 7)	3.04 (m)
6 $\beta$	2.43 (d, 17)	2.42 (d, 17)	2.22 (d, 17)	2.41 (d, 16)	2.36 (d, 16)	2.48 (m)
6 $\alpha$	3.23 (dd, 17, 7)	3.26 (dd, 17, 7)	3.04 (dd, 17, 7)	3.26 (dd, 16, 7)	3.17 (dd, 16, 7)	3.28 (dd, 17, 7)
9	7.51 (br d, 8)	7.49 (br d, 7.5)	7.54 (br d, 7)	7.50 (d, 8)	7.37 (br d, 8)	7.51 (br d, 8)
10	7.13 (td, 8, 1)	7.11 (td, 7.5, 1)	7.17 (m)	7.11 (t, 8)	6.96 (td, 8, 1)	7.13 (td, 8, 1)
11	7.21 (td, 8, 1)	7.20 (td, 7.5, 1)	7.17 (m)	7.20 (t, 8)	7.06 (td, 8, 1)	7.22 (td, 8, 1)
12	7.31 (br d, 8)	7.30 (br d, 7.5)	7.09 (br d, 7)	7.30 (d, 8)	7.20 (br d, 8)	7.31 (br d, 8)
14 $\beta$	1.54 (ddd, 13, 5, 3)	1.53 (m)	1.24 (m)	1.51 (m)	1.46 (m)	1.54 (m)
14 $\alpha$	2.46 (m)	2.45 (m)	2.29 (td, 13, 4)	2.39 (m)	2.31 (m)	2.48 (m)
15	1.85 (dt, 12.7, 5)	1.81 (dt, 13, 5)	1.68 (dt, 13, 5)	1.76 (m)	1.65 (dt, 13, 5)	1.77 (dt, 13, 5)
16	2.10 (m)	2.01 (m)	1.80 (m)	2.15 (m)	2.05 (m)	1.93 (m)
17 $\beta$	3.74 (dd, 12, 5)	3.75 (dd, 12, 5)	3.65 (m)	3.83 (dd, 12, 5)	3.67 (dd, 11, 5)	3.93 (m)
17 $\alpha$	4.08 (t, 12)	4.02 (m)	4.01 (t, 11)	4.06 (t, 12)	3.97 (t, 11)	3.97 (m)
18	1.62 (s)	1.59 (s)	1.62 (s)	1.57 (s)	1.46 (s)	1.62 (s)
20	2.00 (dd, 13, 8)	2.03 (m)	1.94 (m)	1.84 (br t, 10)	1.75 (br t, 10)	2.03 (m)
21	1.75 (dd, 13, 8) ( $\alpha$ )	1.91 (dd, 12, 7) ( $\alpha$ )	1.83 (dd, 13, 8) ( $\alpha$ )	1.97 (dd, 13, 10) ( $\beta$ )	1.86 (dd, 13, 10) ( $\beta$ )	1.96 (dd, 9, 4)
21	2.46 (t, 13) ( $\beta$ )	2.11 (t, 12) ( $\beta$ )	2.08 (t, 13) ( $\beta$ )	2.13 (dd, 13, 9.5) ( $\alpha$ )	2.02 (dd, 13, 9.5) ( $\alpha$ )	2.05 (m)
23	3.77 (m) (ax)	3.60 (m) (eq)	3.67 (m) (eq)	3.39 (br dd, 11, 4) (ax)	3.27 (br dd, 10.5, 3) (ax)	5.11 (dd, 11.5, 5.5)
24ax	1.76 (ddd, 14, 12, 3)	1.91 (m) (eq)	1.76 (m) (eq)	1.60 (q, 11)	1.47 (q, 10.5)	2.16 (m)
24eq	2.10 (m)	2.17 (dt, 14, 3) (ax)	2.06 (m) (ax)	2.15 (m)	2.03 (m)	2.16 (m)
25	3.93 (m) (eq)	3.84 (m) (eq)	3.38 (m) (eq)	3.71 (m)	3.60 (tt, 10.5, 5) (ax)	4.97 (m)
26eq	3.51 (dt, 11, 2)	3.56 (dt, 12, 2.5)	3.34 (dt, 12, 2.5)	3.61 (m)	3.41 (t, 10.5) (ax)	3.59 (br d, 13)
26ax	3.93 (dd, 11, 1)	4.01 (dd, 12, 2)	3.85 (dd, 12, 1.5)	3.69 (m)	3.52 (ddd, 10.5, 5, 1.7) (eq)	3.97 (m)
N(1)-Me	3.63 (s)	3.63 (s)	3.09 (s)	3.61 (s)	3.52 (s)	3.63 (s)
N(4)-Me	2.34 (s)	2.35 (s)	2.20 (s)	2.34 (s)	2.26 (s)	2.42 (s)
23-OH	2.95 (br s)	—	—	—	—	—
23-OAc	—	—	—	—	—	2.09 (s) <sup>d</sup>
25-OAc	—	—	—	—	—	2.11 (s) <sup>d</sup>

eq/ax Assignments of H-24 for compounds **4** and **6** only.

eq/ax Assignments of H-26 for compounds **4** and **5** only.

<sup>a</sup> Measured in  $CDCl_3$ .

<sup>b</sup> Measured in  $C_6D_6/CDCl_3$ .

<sup>c</sup> Measured in  $CD_2Cl_2$ .

<sup>d</sup> Assignments may be reversed.

The proposed structure is in complete agreement with the HMBC data, in particular the observed three-bond correlation from H-26 to C-22 (Fig. 7). The NOE/NOESY data were similar to those obtained for macrodasines A–C (**1**–**3**), confirming the same relative configurations at C-3, C-5, C-15, C-16, C-19, and C-20. This left the configurations of the spirocyclic center C-22 and the stereocenters C-23 and C-25 in the tetrahydropyranyl ring to be determined.

The observed NOE interaction between 18-Me and the H-26 signal at  $\delta$  3.93 (Fig. 8) indicated that this H-26 is axially-oriented in the preferred chair conformation adopted by the tetrahydropyranyl

ring G. This NOE also allowed the assignment of the configuration of the spirocyclic C-22 as *R* (In the case where the C-22 configuration is *S*, the C-26 hydrogens and 18-Me would be directed away from each other and would not be expected to show any NOE). The configurations of the remaining two stereocenters, C-23 and C-25, were assigned through analysis of the coupling constants and from NOE experiments. The attribution of the H-26 resonance at  $\delta$  3.93 to the axially-oriented H-26, allowed assignment of the other H-26 signal at  $\delta$  3.51 to the equatorially-oriented H-26. The axial H-26 was seen as a doublet of doublets with *J* values of 11 and 1 Hz. This means that the adjacent oxymethine H-25 is equatorial, as if H-25 is axial, *trans*-diaxial coupling for H-26/H-25 would have been observed, which was not the case. The signal for the equatorial H-26 is a doublet of triplets, with *J*=11 and 2 Hz ( $J_{26-26}=11$  Hz;  $J_{26-25eq}=J_{26-24eq}=2$  Hz). One of the 2 Hz coupling is a result of long-range *W*-coupling, which was also confirmed by decoupling experiments. The H-24 signal at  $\delta$  1.76 was observed as a ddd (*J*=14, 12, 3 Hz) while the other H-24 was seen as a multiplet at  $\delta$  2.10. The former must be due to the axially-oriented H-24. The oxymethine H-23 at  $\delta$  3.77 was observed as a multiplet in **4**, which in the diacetate derivative **12** resolved into a doublet of doublets at  $\delta$  5.11 ( $J_{23-24ax}=11.5$  Hz,  $J_{23-24eq}=5.5$  Hz). Hydrogen-23 in **12** (and **4**)

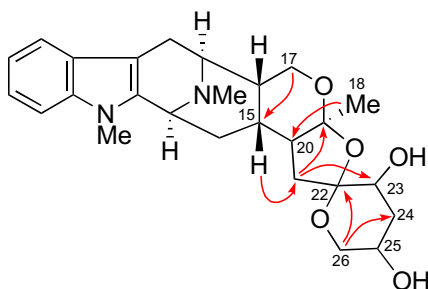
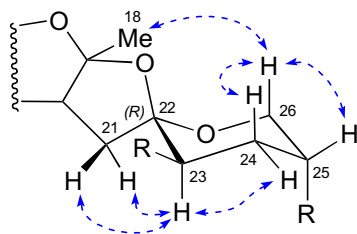
must therefore also be axially-oriented. These assignments are also consistent with the observed H-24ax/H-26ax, H-25eq, and H-23/H-21 $\beta$ , H-21 $\alpha$  NOEs. Based on these observations, the configurations at C-23 and C-25 are assigned as 23*R* and 25*R*, respectively.

Macrodasine E (**5**) was obtained as a light yellowish oil with  $[\alpha]_D^{25} +20$  (c 0.28,  $CHCl_3$ ). The UV, IR, MS, and NMR data were similar to those of macrodasine D (**4**) indicating a similar structure with a six-membered ring G, in the form of a tetrahydropyranyl ring substituted by two hydroxyl groups. This was also confirmed by the observed three-bond H-26 to C-22 correlation in the HMBC



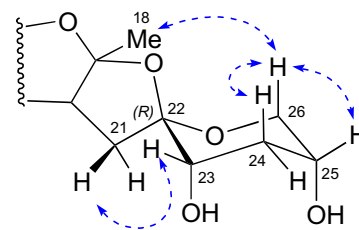
**Table 3**<sup>13</sup>C (100 MHz) NMR data of **1–7** and **9–12** in CDCl<sub>3</sub><sup>a</sup>

C	1	2	3	4	5	6	7	9	10	11	12
2	132.8	131.5	132.7	<sup>b</sup>	132.4	132.7	132.5	132.5	132.9	<sup>b</sup>	132.6
3	53.3	53.3	53.2	53.6	53.2	53.3	53.3	53.3	53.7	53.5	53.3
5	54.8	54.7	55.4	54.8	55.2	54.9	54.7	55.0	55.0	54.7	56.2
6	22.5	22.6	22.3	22.5	22.3	22.4	22.5	22.7	22.9	22.7	22.7
7	106.4	106.5	106.6	106.4	106.3 <sup>c</sup>	106.6 <sup>c</sup>	106.5	106.4	106.9	106.7	106.4 <sup>c</sup>
8	126.4	126.2	126.3	126.1	126.1	126.3	126.2	126.2	126.6	126.4	126.3
9	118.0	118.0	118.1	118.1	117.9	118.0	118.0	118.1	118.3	118.2	118.2
10	118.9	118.9	118.9	119.2	118.8	118.9	118.9	119.0	119.2	119.1	119.1
11	121.0	121.0	121.0	121.1	120.8	120.9	121.0	121.1	121.2	121.2	121.2
12	108.0	108.8	108.8	108.8	108.6	108.8	108.8	108.9	109.0	109.0	108.9
13	136.9	137.1	136.9	137.0	136.8	136.9	136.9	137.0	137.2	137.1	137.1
14	31.9	31.9	32.2	31.6	32.0	32.1	31.9	31.9	32.3	31.9	32.4
15	26.5	27.1	26.7	26.2	26.2	27.2	27.0	27.0	27.1	26.5	26.2
16	36.9	36.6	36.0	36.8	36.6	36.4	36.5	36.9	37.0	36.9	36.8
17	64.3	64.8	64.8	64.2	64.0	64.5	64.7	64.3	64.9	64.5	63.7
18	24.2	23.5	25.9	23.8	25.0	24.1	23.6	23.9	23.4	23.8	26.5
19	105.5	106.1	106.8	105.4	106.1 <sup>c</sup>	106.5 <sup>c</sup>	105.3	104.9	105.4	105.0	106.3 <sup>c</sup>
20	44.3	45.8	44.2	43.6	43.2	46.0	45.6	45.1	45.2	44.8	42.5
21	34.7	35.9	35.6	36.9	38.2	39.8	38.2	33.0	39.6	35.7	36.6
22	114.8	106.4	104.2	106.6	105.6	105.3	112.0	116.6	111.9	111.5	103.8
23	77.7	209.4	207.1	64.1	70.2	70.1	75.7	74.1	76.6	74.3	66.7
24	33.0	34.7	34.0	36.1	32.4	37.9	34.2	34.3	32.1	31.6	29.1
25	79.2	75.0	75.5	67.1	65.1	65.0	77.0	76.9	74.6	77.7	69.4
26	63.9	63.1	64.0	65.5	66.1	66.6	64.6	63.3	65.9	64.0	62.4
N(1)-Me	29.0	29.0	29.0	29.0	28.8	29.0	29.0	29.0	29.3	29.2	29.7
N(4)-Me	41.6	41.7	41.8	41.5	41.6	41.7	41.6	41.6	42.0	41.8	41.8
23-OAc	—	—	—	—	—	—	—	—	21.2	—	21.3 <sup>c</sup>
25-OAc	—	—	—	—	—	—	—	—	170.9	—	170.6 <sup>c</sup>
									21.2	—	21.4 <sup>c</sup>
									171.1	—	170.8 <sup>c</sup>

<sup>a</sup> Assignments based on COSY, HMQC, HETCOR, and HMBC.<sup>b</sup> Not detected.<sup>c</sup> Assignments may be reversed.**Fig. 7.** Selected HMBCs of **4**.**Fig. 8.** Selected NOEs of **4** (R=OH).

spectrum. As in the preceding compound **4**, the configurations of the spirocyclic center C-22, and the stereocenters C-23 and C-25 in the tetrahydropyranyl ring, were determined by analysis of the coupling constants and from NOE/NOESY experiments. As with **4**, the observed NOE between 18-Me/H-26ax allowed the configuration of the spirocenter at C-22 to be assigned as *R*. The <sup>1</sup>H NMR spectrum (Table 2) of **5** in CDCl<sub>3</sub> showed overlap of the H-17 $\alpha$  and H-26ax signals ( $\delta$  4.01–4.02, 2H). Fortunately these signals were

resolved when the <sup>1</sup>H NMR spectrum (Table 2) was recorded in C<sub>6</sub>D<sub>6</sub> with a few drops of CDCl<sub>3</sub> added ( $\delta$  4.01, t, *J*=11 Hz, H-17 $\alpha$ ;  $\delta$  3.85, dd, *J*=12, 1.5 Hz, H-26ax). The use of C<sub>6</sub>D<sub>6</sub>/CDCl<sub>3</sub> as solvent for NMR has therefore allowed clear observation of both the 18-Me/H-17 $\alpha$ , H-26ax, as well as the H-23eq/H-21 $\beta$  NOEs, which are consistent with the assignment of the C-22 spirocyclic center as *R* (Fig. 9).

**Fig. 9.** Selected NOEs of **5**.

The assignment of the oxymethine C-23 and C-25 configurations were carried out following the same approach as that used in the case of **4** above, i.e., via analysis of the coupling constants and from the NOE data (in C<sub>6</sub>D<sub>6</sub>/CDCl<sub>3</sub> unless otherwise stated). As in **4**, the axially-oriented H-26 (from the 18-Me/H-26ax NOE) was in **5** observed at  $\delta$  3.85 as a doublet of doublets (*J*<sub>26–26eq</sub>=12 Hz, *J*<sub>26ax–25eq</sub>=2 Hz), which in turn indicated that H-25 was equatorial. The observed reciprocal NOEs between the axial H-26 and the H-24 signal at  $\delta$  2.06 require these hydrogens to be in a 1,3-diaxial relationship in the preferred chair conformation adopted by the six-membered ring. The other H-24 signal at  $\delta$  1.76 is therefore due to the equatorially-oriented hydrogen. Both these H-24 signals were seen as multiplets in C<sub>6</sub>D<sub>6</sub>/CDCl<sub>3</sub>, whereas in CDCl<sub>3</sub>, while the equatorial H-24 signal remained as a multiplet, the axial H-24 was observed as a doublet of triplets (*J*<sub>24–24</sub>=14 Hz; *J*<sub>24ax–25eq</sub>=*J*<sub>24ax–23eq</sub>=3 Hz). The observed

coupling behavior is thus consistent with the assignment of both H-23 and H-25 as having an equatorial orientation (or C-23S and C-25R). In the case of **4**, the axially-oriented H-23 showed NOE interactions with both H-21 $\alpha$  and H-21 $\beta$ . In **5** on the other hand, the equatorially-oriented H-23 showed NOE interaction with H-21 $\beta$  only, providing additional support for the equatorial orientation of H-23. Compound **5** is therefore the C-23S epimer of macrodasine D (**4**).

Macrodasine F (**6**) was obtained as a light yellowish oil with  $[\alpha]_D^{25} -51$  (c 0.40, CHCl<sub>3</sub>). The UV, IR, MS, and NMR data were similar to those of macrodasines D (**4**) and E (**5**) indicating that **4**, **5**, and **6** are stereoisomers. In the case of **6**, it was found that the use of CD<sub>2</sub>Cl<sub>2</sub> was best suited for the extensive NOE experiments required as it provided clear and well resolved signals for the hydrogens on C-25, C-26, and N(1)-Me, compared to spectra obtained in CDCl<sub>3</sub>. In the previous two alkaloids, **4** and **5**, the observed NOE between 18-Me and the axial H-26 was diagnostic of C-22R configuration. In the present compound **6**, NOE was not observed between the C-26 hydrogens and 18-Me, suggesting that the configuration of the spirocyclic C-22 is *S* (the C-26 hydrogens and 18-Me are directed away from each other). Instead, in the case of **6**, NOE was observed between the oxymethine H-23 and H-21 $\alpha$  (Fig. 10). Examination of models showed that this is only possible when the C-22 configuration is *S* and H-23 is axially-oriented. This NOE therefore allowed the simultaneous assignment of both the spirocyclic C-22 and the oxymethine C-23 as *S* (H-23 axial). Irradiation of H-23 also resulted in the enhancement of the oxymethine H-25 signal at  $\delta$  3.60 and vice versa. Since H-23 is axial, this NOE requires H-25 to be axial as well (1,3-diaxial arrangement of H-23 and H-25 in the preferred chair conformation for the tetrahydropyranyl ring G), leading to the assignment of C-25 as *R*. These conclusions are also entirely consistent with the observed vicinal coupling constants. The axially-oriented H-23 was seen at  $\delta$  3.27 as a doublet of doublets ( $J=10.5, 3$  Hz). This is coupled to the axial H-24, which was seen as a quartet ( $J=10.5$  Hz) at  $\delta$  1.47. This requires  $J_{24ax-23ax}=J_{24-24}=J_{24ax-25ax}=10.5$  Hz, which is consistent with the equatorial orientation of the C(25)-OH (or C-25R). In addition, the observed NOE between H-24ax ( $\delta$  1.47) and the H-26 signal at  $\delta$  3.41 indicated that this H-26 is axially-oriented, which is consistent with the observed coupling pattern for the H-26 resonance (t,  $J=10.5$  Hz; i.e.,  $J_{26-26}=J_{26ax-25ax}=10.5$  Hz). In addition, this coupling behavior is also in agreement with the presence of an equatorially-oriented OH at C-25. The signal due to H-25ax ( $\delta$  3.60) was seen as a triplet of triplets with  $J=10.5$  and 5 Hz ( $J_{25ax-26ax}=J_{25ax-24ax}=10.5$  Hz;  $J_{25ax-26eq}=J_{25ax-24eq}=5$  Hz) while the equatorial H-26 at  $\delta$  3.52 (ddd,  $J=10.5, 5, 1.7$  Hz) showed in addition to geminal coupling, and coupling to H-25ax, evidence of long-range W-coupling (1.7 Hz) to the equatorial H-24 at  $\delta$  2.03.

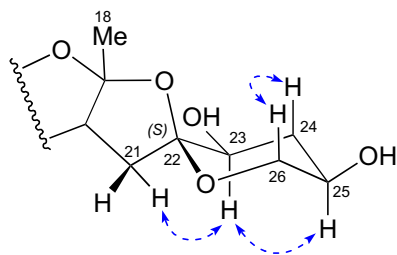


Fig. 10. Selected NOEs of **6**.

Macrodasine G was obtained as a light yellowish oil, with  $[\alpha]_D^{25} -59$  (c 0.27, CHCl<sub>3</sub>). The UV and IR spectra were similar to those of macrodasine A (**1**), indicating the presence of similar functionalities. The EIMS showed a molecular ion peak at  $m/z$  454, and HREIMS measurements gave the molecular formula C<sub>26</sub>H<sub>34</sub>N<sub>2</sub>O<sub>5</sub>, indicated that macrodasine G was isomeric with **1**. The NMR data

showed a close resemblance to those of **1**, except for minor variations in the chemical shifts involving the rings F and G. Examination of NMR data of macrodasine G showed that it corresponded to those of compound **7**, the major product (epimer) from NaBH<sub>4</sub> reduction of macrodasine B (**2**). Macrodasine G (**7**) is therefore the 22(*S*) diastereomer of macrodasine A (**1**).

The macrodasines A–G (**1–7**), represent the first members of an unusual class of macroline compounds, which have incorporated additional novel structural features, in the form of fused spirocyclic tetrahydrofuran–tetrahydrofuran and tetrahydrofuran–tetrahydropyran rings. Compounds **2**, **3**, and **5** were found to show moderate levels of activity in reversing multidrug-resistance in drug-resistant KB cells (KB/VJ300)<sup>36</sup> with IC<sub>50</sub> values of 12.8, 6.7, and 11.8  $\mu$ g/mL, respectively.

### 3. Experimental

#### 3.1. General

Optical rotations were determined on a JASCO P-1020 digital polarimeter. IR spectra were recorded on a Perkin–Elmer RX1 FT-IR spectrophotometer. UV spectra were obtained on a Shimadzu UV-3101PC spectrophotometer. <sup>1</sup>H and <sup>13</sup>C NMR spectra were recorded in CDCl<sub>3</sub>, CD<sub>2</sub>Cl<sub>2</sub>, and C<sub>6</sub>D<sub>6</sub> using TMS as an internal standard on JEOL JNM-LA 400 and JNM-ECA 400 spectrometers at 400 and 100 MHz, respectively. X-ray diffraction analysis was carried out on a Bruker SMART APEX II CCD area detector system equipped with a graphite monochromator and a Mo K $\alpha$  fine-focus sealed tube ( $\lambda=0.71073$  Å), at 100 K. The structure was solved by direct methods (SHELXS-97) and refined with full-matrix least squares on *F*<sup>2</sup> (SHELXL-97). EIMS and HREIMS were obtained at Organic Mass Spectrometry, Central Science Laboratory, University of Tasmania, Tasmania, Australia. All air-moisture-sensitive reactions were carried out under N<sub>2</sub> in oven-dried glassware. MeOH was freshly distilled from magnesium turnings. All other reagents were used without further purification.

#### 3.2. Plant material and extraction of alkaloids

Plant material was collected in Johor, Malaysia (June 2003) and was identified by Professor K. M. Wong, Institute of Biological Sciences, University of Malaya, Malaysia. Herbarium voucher specimens (K665) are deposited at the Herbarium of the University of Malaya. The ground stem-bark material was extracted with EtOH and the concentrated EtOH extract was then partitioned with dilute acid to provide a basic fraction, as has been described in detail elsewhere.<sup>37</sup>

#### 3.3. Isolation

The alkaloids were isolated by initial column chromatography on silica gel using CHCl<sub>3</sub> with increasing proportions of MeOH followed by rechromatography of the appropriate partially resolved fractions using centrifugal TLC. Solvent systems used for centrifugal TLC were Et<sub>2</sub>O, Et<sub>2</sub>O/MeOH (25:2) (NH<sub>3</sub>-saturated), CHCl<sub>3</sub>/hexane (NH<sub>3</sub>-saturated) (1:1), CHCl<sub>3</sub>/MeOH (100:1), CHCl<sub>3</sub> (NH<sub>3</sub>-saturated), and EtOAc/hexane (NH<sub>3</sub>-saturated). The yields (g kg<sup>-1</sup>) of the alkaloids were as follows: **1** (0.003), **2** (0.006), **3** (0.002), **4** (0.001), **5** (0.0007), **6** (0.001), and **7** (0.002).

**3.3.1. Macrodasine A (1).** Colorless plates from ethanol; mp 149–154 °C;  $[\alpha]_D^{25} +36$  (c 0.36, CHCl<sub>3</sub>); UV (EtOH)  $\lambda_{max}$  (log  $\epsilon$ ) 230 (3.88), 287 (3.17) nm; IR (dry film)  $\nu_{max}$  3411 cm<sup>-1</sup>; <sup>1</sup>H NMR (400 MHz, CDCl<sub>3</sub>, and CD<sub>2</sub>Cl<sub>2</sub>), see Table 1; <sup>13</sup>C NMR (100 MHz, CDCl<sub>3</sub>), see Table 3; EIMS  $m/z$  (rel int) 454 [M]<sup>+</sup> (78), 439 (4), 424 (44), 367 (7), 197 (100), 182 (27), 181 (16), 170 (34), 144 (13), 70 (26),

57 (16), 43 (36); HREIMS  $m/z$  454.2462 (calcd for  $C_{26}H_{34}N_2O_5$   $[M]^+$ , 454.2468).

**3.3.2. Macrodasine B (2).** Light yellowish oil;  $[\alpha]_D^{25} +149$  (c 0.07,  $CHCl_3$ ); UV (EtOH)  $\lambda_{max}$  (log  $\epsilon$ ) 230 (3.95), 287 (3.23) nm; IR (dry film)  $\nu_{max}$  1765, 3435  $cm^{-1}$ ;  $^1H$  NMR (400 MHz,  $CDCl_3$ ), see Table 1;  $^{13}C$  NMR (100 MHz,  $CDCl_3$ ), see Table 3; EIMS  $m/z$  452  $[M]^+$  (64), 437 (3), 421 (12), 366 (11), 322 (17), 293 (4), 237 (6), 197 (100), 182 (26), 181 (19), 170 (29), 144 (9), 85 (13), 70 (19), 57 (16), 40 (35); HREIMS  $m/z$  452.2326 (calcd for  $C_{26}H_{32}N_2O_5$   $[M]^+$ , 452.2311).

**3.3.3.  $NaBH_4$  reduction of macrodasine B (2).** To a mixture of ketone **2** (17 mg, 0.038 mmol) in 5 mL of MeOH at 3 °C was added  $NaBH_4$  (1.7 mg, 0.045 mmol) and the solution was stirred for 15 min. Excess solvent was removed under reduced pressure. Saturated  $NH_4Cl$  solution (10 mL) was then added and the mixture was extracted with  $CH_2Cl_2$  ( $3 \times 10$  mL), dried ( $Na_2SO_4$ ), and then chromatographed ( $SiO_2$ , centrifugal TLC, 3% MeOH/ $CH_2Cl_2$ ) to give a mixture comprising the alcohols, **7** {major epimer} (11.8 mg, 69%) and **9** {minor epimer} (1.9 mg, 11%), and unreacted macrodasine B (**2**) (1 mg, 5.9%). Compound **9**: colorless oil;  $[\alpha]_D^{25} -60$  (c 0.13,  $CHCl_3$ ); UV (EtOH)  $\lambda_{max}$  (log  $\epsilon$ ) 229 (4.52), 286 (3.81) nm; IR (dry film)  $\nu_{max}$  3358  $cm^{-1}$ ;  $^1H$  NMR (400 MHz,  $CDCl_3$ ), see Table 1;  $^{13}C$  NMR (100 MHz,  $CDCl_3$ ), see Table 3; EIMS  $m/z$  454  $[M]^+$  (21), 436 (4), 423 (8), 394 (5), 367 (3), 321 (6), 321 (6), 282 (5), 267 (8), 237 (6), 197 (100), 170 (42), 144 (13), 128 (7), 83 (6), 70 (14), 57 (6), 44 (14); HREIMS  $m/z$  454.2464 (calcd for  $C_{26}H_{34}N_2O_5$   $[M]^+$ , 454.2468).

**3.3.4. Macrodasine C (3).** Light yellowish oil;  $[\alpha]_D^{25} -45$  (c 0.14,  $CHCl_3$ ); UV (EtOH)  $\lambda_{max}$  (log  $\epsilon$ ) 229 (4.46), 286 (3.77) nm; IR (dry film)  $\nu_{max}$  3467, 1766  $cm^{-1}$ ;  $^1H$  NMR (400 MHz,  $CDCl_3$ ), see Table 1;  $^{13}C$  NMR (100 MHz,  $CDCl_3$ ), see Table 3; EIMS  $m/z$  452  $[M]^+$  (35), 421 (11), 366 (15), 322 (11), 237 (5), 197 (100), 170 (26), 144 (8), 70 (17), 49 (17); HREIMS  $m/z$  452.2315 (calcd for  $C_{26}H_{32}N_2O_5$   $[M]^+$ , 452.2311).

**3.3.5.  $NaBH_4$  reduction of macrodasine C (3).** To a mixture of ketone **3** (10 mg, 0.022 mmol) in 5 mL of MeOH at 3 °C was added  $NaBH_4$  (1.0 mg, 0.026 mmol) and the solution was stirred for 15 min. Excess solvent was removed under reduced pressure. Saturated  $NH_4Cl$  solution (10 mL) was then added and the mixture was extracted with  $CH_2Cl_2$  ( $3 \times 10$  mL), dried ( $Na_2SO_4$ ), and then chromatographed ( $SiO_2$ , centrifugal TLC, 2% MeOH/EtOAc,  $NH_3$ -saturated) to give a mixture comprising the alcohol **11** (3.6 mg, 36%) and unreacted macrodasine C (**3**) (1 mg, 10%). Compound **11**: light yellowish oil;  $[\alpha]_D^{25} -6$  (c 0.06,  $CHCl_3$ ); UV (EtOH)  $\lambda_{max}$  (log  $\epsilon$ ) 228 (4.39), 286 (3.72) nm; IR (dry film)  $\nu_{max}$  3439  $cm^{-1}$ ;  $^1H$  NMR (400 MHz,  $CDCl_3$ ), see Table 1;  $^{13}C$  NMR (100 MHz,  $CDCl_3$ ), see Table 3; EIMS  $m/z$  454  $[M]^+$  (17), 436 (3), 423 (8), 394 (4), 367 (3), 321 (5), 278 (2), 237 (5), 197 (100), 170 (48), 144 (10), 129 (7), 83 (7), 70 (15), 44 (30); HREIMS  $m/z$  454.2465 (calcd for  $C_{26}H_{34}N_2O_5$ , 454.2468).

**3.3.6. Macrodasine D (4).** Colorless oil;  $[\alpha]_D^{25} -12$  (c 0.10,  $CHCl_3$ ); UV (EtOH)  $\lambda_{max}$  (log  $\epsilon$ ) 229 (4.20), 286 (3.47) nm; IR (dry film)  $\nu_{max}$  3420  $cm^{-1}$ ;  $^1H$  NMR (400 MHz,  $CDCl_3$ ), see Table 2;  $^{13}C$  NMR (100 MHz,  $CDCl_3$ ), see Table 1; EIMS  $m/z$  454  $[M]^+$  (28), 423 (5), 367 (19), 354 (2), 322 (5), 293 (3), 251 (5), 237 (8), 211 (11), 197 (100), 182 (32), 181 (21), 170 (40), 144 (14), 128 (7), 98 (5), 70 (13), 44 (14); HREIMS  $m/z$  454.2464 (calcd for  $C_{26}H_{34}N_2O_5$   $[M]^+$ , 454.2468).

**3.3.7. Acetylation of macrodasine D (4).** Macrodasine D (**4**) (4.5 mg, 0.010 mmol) was added to a mixture of acetic anhydride/pyridine (1:1; 1 mL) and the mixture stirred under  $N_2$  at room temperature for 2 h 30 min, after which a further portion of DMAP (0.12 mg, 0.001 mmol) was added, and the mixture stirred for another 30 min. The mixture was then poured into saturated  $Na_2CO_3$

solution (5 mL) and extracted with  $CH_2Cl_2$  ( $3 \times 5$  mL). Removal of the solvent, followed by purification by centrifugal TLC over  $SiO_2$  (2% MeOH/EtOAc) afforded 3 mg (56%) of the diacetate derivative **12** as a colorless oil;  $[\alpha]_D^{25} +12$  (c 0.095,  $CHCl_3$ ); UV (EtOH)  $\lambda_{max}$  (log  $\epsilon$ ) 230 (4.23), 288 (3.39) nm; IR (dry film)  $\nu_{max}$  1738  $cm^{-1}$ ;  $^1H$  NMR (400 MHz,  $CDCl_3$ ), see Table 2;  $^{13}C$  NMR (100 MHz,  $CDCl_3$ ), see Table 3; EIMS  $m/z$  538  $[M]^+$  (87), 495  $[M-COMe]^+$  (25), 479  $[M-OCOMe]^+$  (10), 448 (2), 409 (3), 367 (5), 350 (17), 322 (8), 290 (4), 237 (8), 197 (100), 182 (21), 170 (23), 144 (12), 70 (13), 43 (17); HREIMS  $m/z$  538.2681 (calcd for  $C_{30}H_{38}N_2O_7$   $[M]^+$ , 538.2679).

**3.3.8. Macrodasine E (5).** Colorless oil;  $[\alpha]_D^{25} +20$  (c 0.28,  $CHCl_3$ ); UV (EtOH)  $\lambda_{max}$  (log  $\epsilon$ ) 230 (3.50), 289 (2.55) nm; IR (dry film)  $\nu_{max}$  3436  $cm^{-1}$ ;  $^1H$  NMR (400 MHz,  $CDCl_3$ , and  $C_6D_6/CDCl_3$ ), see Table 2;  $^{13}C$  NMR (100 MHz,  $CDCl_3$ ), see Table 3; EIMS  $m/z$  454  $[M]^+$  (73), 436  $[M-H_2O]^+$  (6), 423 (15), 394 (5), 367 (19), 197 (100), 182 (31), 181 (17), 170 (39), 144 (14), 70 (23), 57 (7), 43 (13); HREIMS  $m/z$  454.2473 (calcd for  $C_{26}H_{34}N_2O_5$   $[M]^+$ , 454.2468).

**3.3.9. Macrodasine F (6).** Colorless oil;  $[\alpha]_D^{25} -51$  (c 0.40,  $CHCl_3$ ); UV (EtOH)  $\lambda_{max}$  (log  $\epsilon$ ) 229 (4.52), 287 (3.77) nm; IR (dry film)  $\nu_{max}$  3394  $cm^{-1}$ ;  $^1H$  NMR (400 MHz,  $CDCl_3$ , and  $CD_2Cl_2$ ), see Table 2;  $^{13}C$  NMR (100 MHz,  $CDCl_3$ ), see Table 3; EIMS  $m/z$  454  $[M]^+$  (58), 436  $[M-H_2O]^+$  (6), 423 (10), 394 (4), 367 (29), 351 (2), 321 (8), 277 (4), 237 (8), 197 (100), 182 (23), 181 (14), 170 (35), 129 (5), 97 (5), 70 (15), 57 (7), 43 (12); HREIMS  $m/z$  454.2468 (calcd for  $C_{26}H_{34}N_2O_5$   $[M]^+$ , 454.2468).

**3.3.10. Macrodasine G (7).** Colorless oil;  $[\alpha]_D^{25} -59$  (c 0.27,  $CHCl_3$ ); UV (EtOH)  $\lambda_{max}$  (log  $\epsilon$ ) 206 (4.50), 229 (4.50), 286 (3.79) nm; IR (dry film)  $\nu_{max}$  3424  $cm^{-1}$ ;  $^1H$  NMR (400 MHz,  $CDCl_3$ ), see Table 1;  $^{13}C$  NMR (100 MHz,  $CDCl_3$ ), see Table 3; EIMS  $m/z$  454  $[M]^+$  (40), 436 (5), 423 (12), 394 (6), 367 (3), 321 (7), 277 (3), 237 (6), 197 (100), 170 (44), 144 (10), 128 (7), 98 (5), 70 (13), 55 (5), 44 (20); HREIMS  $m/z$  454.2469 (calcd for  $C_{26}H_{34}N_2O_5$   $[M]^+$ , 454.2468).

**3.3.11. Acetylation of macrodasine G (7).** Macrodasine G (**7**) (9.7 mg, 0.021 mmol) was added to a mixture of acetic anhydride/pyridine (1:1; 1 mL) and the mixture stirred under  $N_2$  at room temperature for 2 h. The mixture was then poured into saturated  $Na_2CO_3$  solution (5 mL) and extracted with  $CH_2Cl_2$  ( $3 \times 5$  mL). Removal of the solvent, followed by purification by centrifugal TLC over  $SiO_2$  (2% MeOH/ $CH_2Cl_2$ ) afforded 6 mg (52%) of the diacetate derivative **10**. Compound **10**: colorless needles from ethanol, mp 186–188 °C;  $[\alpha]_D^{25} -46$  (c 0.09,  $CHCl_3$ ); IR (dry film)  $\nu_{max}$  1738  $cm^{-1}$ ; UV (EtOH)  $\lambda_{max}$  (log  $\epsilon$ ) 203 (3.86), 230 (3.86), 254 (3.67), 286 (3.14) nm;  $^1H$  NMR (400 MHz,  $CDCl_3$ ), see Table 1;  $^{13}C$  NMR (100 MHz,  $CDCl_3$ ), see Table 3; EIMS  $m/z$  538  $[M]^+$  (55), 495 (14), 465 (11), 393 (5), 350 (4), 307 (4), 277 (5), 251 (8), 197 (100), 182 (23), 144 (13), 129 (4), 98 (3), 70 (11), 55 (3), 43 (19); HREIMS  $m/z$  538.2678 (calcd for  $C_{30}H_{38}N_2O_7$   $[M]^+$ , 538.2679).

### 3.4. X-ray crystallographic analysis of 1

A single crystal of **1** was obtained from ethanol;  $C_{26}H_{34}N_2O_5 \cdot 5H_2O$ ,  $M_r=544.63$ , monoclinic, space group  $P2_1$ ,  $a=7.5783$  (3) Å,  $b=9.2235$  (4) Å,  $c=19.5949$  (9) Å,  $\beta=92.252$  (3)°;  $V=1368.6$  (10) Å<sup>3</sup>,  $Z=2$ ,  $D_{calcd}=1.322$   $cm^{-3}$ . The structure was solved by direct methods and refined by the least squares method. The final  $R$  value is 0.0709 ( $R_w=0.1974$ ) for 5046 reflections [ $I>2\sigma(I)$ ].

A single crystal of **10** was obtained from ethanol;  $C_{30}H_{38}N_2O_7$ ,  $M_r=538.62$ , orthorhombic, space group  $P2_12_12_1$ ,  $a=7.626$  (5) Å,  $b=17.595$  (10) Å,  $c=20.657$  (15) Å,  $V=2771.8$  (3) Å<sup>3</sup>,  $Z=4$ ,  $D_{calcd}=1.291$   $cm^{-3}$ . The structure was solved by direct methods and refined by the least squares method. The final  $R$  value is 0.0628 ( $R_w=0.1791$ ) for 2428 reflections [ $I>2\sigma(I)$ ].



Crystallographic data for the structures **1** and **10** reported in this paper have been deposited with the Cambridge Crystallographic Data Center (deposition number: CCDC 806140 and 806141, respectively). Copies of the data can be obtained, free of charge, on application to the Director, CCDC, 12 Union Road, Cambridge CB2 1EZ, UK (fax: +44 (0) 1223 336033 or e-mail: [deposit@ccdc.cam.ac.uk](mailto:deposit@ccdc.cam.ac.uk)).

### 3.5. Cytotoxicity assays

Cytotoxicity assays were carried out following the procedure that has been described previously.<sup>38,39</sup>

### Acknowledgements

We would like to thank the University of Malaya (UMRG, HIR-Grant) and MOHE Malaysia (FRGS) for financial support.

### Supplementary data

Supplementary data related to this article can be found online at [doi:10.1016/j.tet.2011.03.099](https://doi.org/10.1016/j.tet.2011.03.099).

### References and notes

- Sidiyasa, K. *Taxonomy, Phylogeny, and Wood Anatomy of Alstonia (Apocynaceae)*. Blumea; Rijksherbarium/Hortus Botanicus: The Netherlands, 1998; Supplement 11, pp 1–230.
- Hamaker, L. K.; Cook, J. M. In *Alkaloids: Chemical and Biological Perspectives*; Pelletier, S. W., Ed.; Pergamon: London, 1994; Vol. 9, pp 23–84.
- Kam, T. S. In *Alkaloids: Chemical and Biological Perspectives*; Pelletier, S. W., Ed.; Elsevier: Oxford, 1999; Vol. 14, pp 285–435.
- Kam, T. S.; Choo, Y. M. In *The Alkaloids*; Cordell, G. A., Ed.; Academic: Amsterdam, 2006; Vol. 63, pp 181–337.
- Kam, T. S.; Tan, S. J.; Ng, S. W.; Komiyama, K. *Org. Lett.* **2008**, *10*, 3749.
- Keawpradub, N.; Kirby, G. C.; Steele, J. C. P.; Houghton, P. J. *Planta Med.* **1999**, *65*, 690.
- Keawpradub, N.; Eno-Amooquaye, E.; Burke, P. J.; Houghton, P. J. *Planta Med.* **1999**, *65*, 311.
- Keawpradub, N.; Houghton, P. J.; Eno-Amooquaye, E.; Burke, P. J. *Planta Med.* **1997**, *63*, 97.
- Wright, C. W.; Allen, D.; Phillipson, J. D.; Kirby, G. C.; Warhurst, D. C.; Massiot, G.; Le Men-Olivier, L. *J. Ethnopharmacol.* **1993**, *40*, 41.
- Wright, C. W.; Allen, D.; Cai, Y.; Phillipson, J. D.; Said, I. M.; Kirby, G. C.; Warhurst, D. C. *Phytother. Res.* **1992**, *6*, 121.
- Carroll, A. R.; Hyde, E.; Smith, J.; Quinn, R. J.; Guymer, G.; Forster, P. I. *J. Org. Chem.* **2005**, *70*, 1096.
- Tan, S. J.; Low, Y. Y.; Choo, Y. M.; Abdullah, Z.; Etoh, T.; Hayashi, M.; Komiyama, K.; Kam, T. S. *J. Nat. Prod.* **2010**, *73*, 1891.
- Tan, S. J.; Choo, Y. M.; Thomas, N. F.; Robinson, W. T.; Komiyama, K.; Kam, T. S. *Tetrahedron* **2010**, *66*, 7799.
- Kam, T. S.; Choo, Y. M.; Komiyama, K. *Tetrahedron* **2004**, *60*, 3957.
- Kam, T. S.; Choo, Y. M. *J. Nat. Prod.* **2004**, *67*, 547.
- Kam, T. S.; Choo, Y. M. *Phytochemistry* **2004**, *65*, 603.
- Kam, T. S.; Choo, Y. M. *Helv. Chim. Acta* **2004**, *87*, 366.
- Kam, T. S.; Choo, Y. M. *Tetrahedron Lett.* **2003**, *44*, 8787.
- Kam, T. S.; Choo, Y. M. *Tetrahedron* **2000**, *56*, 6143.
- Kam, T. S.; Iek, I. H.; Choo, Y. M. *Phytochemistry* **1999**, *51*, 839.
- Macabeo, A. P. G.; Krohn, K.; Gehle, D.; Read, R. W.; Brophy, J. J.; Cordell, G. A.; Franzblau, S. G.; Aguinaldo, A. M. *Phytochemistry* **2005**, *66*, 1158.
- Koyama, K.; Hirasawa, Y.; Nugroho, A. E.; Hosoya, T.; Hoe, T. C.; Chan, K. L.; Morita, H. *Org. Lett.* **2010**, *12*, 4188.
- Wang, F.; Ren, F. C.; Liu, J. K. *Phytochemistry* **2009**, *70*, 650.
- Cai, X. H.; Du, Z. Z.; Luo, X. D. *Org. Lett.* **2007**, *9*, 1817.
- Koyama, K.; Hirasawa, Y.; Zaima, K.; Hoe, T. C.; Chan, K. L.; Morita, H. *Bioorg. Med. Chem.* **2008**, *16*, 6483.
- Cai, X. H.; Tan, Q. G.; Liu, Y. P.; Feng, T.; Du, Z. Z.; Li, W. Q.; Luo, X. D. *Org. Lett.* **2008**, *10*, 577.
- Hirasawa, Y.; Arai, H.; Zaima, K.; Oktarina, R.; Rahman, A.; Ekasari, W.; Widayawaruyanti, A.; Indrayanto, G.; Zaini, N. C.; Morita, H. *J. Nat. Prod.* **2009**, *72*, 304.
- Feng, T.; Li, Y.; Cai, X. H.; Gong, X.; Liu, Y. P.; Zhang, R. T.; Zhang, X. Y.; Tan, Q. G.; Luo, X. D. *J. Nat. Prod.* **2009**, *72*, 1836.
- Hirasawa, Y.; Miyama, S.; Kawahara, N.; Goda, Y.; Rahman, A.; Ekasari, W.; Widayawaruyanti, A.; Indrayanto, G.; Zaini, N. C.; Morita, H. *Heterocycles* **2009**, *79*, 1107.
- Feng, T.; Cai, X. H.; Zhao, P. J.; Du, Z. Z.; Li, W. Q.; Luo, X. D. *Planta Med.* **2009**, *75*, 1537.
- Arai, H.; Hirasawa, Y.; Rahman, A.; Kusumawati, I.; Zaini, N. C.; Sato, S.; Aoyama, C.; Takeo, J.; Morita, H. *Bioorg. Med. Chem.* **2010**, *18*, 2152.
- Zuo, H.; He, H. P.; Lou, X. D.; Wang, Y. H.; Yang, X. W.; Di, Y. T.; Hoa, X. J. *Helv. Chim. Acta* **2005**, *88*, 2508.
- Koyama, K.; Hirasawa, Y.; Hosoya, T.; Hoe, T. C.; Chan, K. L.; Morita, H. *Bioorg. Med. Chem.* **2010**, *18*, 4415.
- Mayerl, F.; Hesse, M. *Helv. Chim. Acta* **1978**, *61*, 337.
- (a) Hirotsu, M.; Sai, K.; Hirotsu, S.; Yoshikawa, T. *Phytochemistry* **2002**, *59*, 571; (b) Liu, H.; Chou, G. X.; Wu, T.; Guo, Y. L.; Wang, S. C.; Wang, C. H.; Wang, Z. T. *J. Nat. Prod.* **2009**, *72*, 1964.
- Kam, T. S.; Subramaniam, G.; Sim, K. M.; Yoganathan, K.; Koyano, T.; Toyoshima, M.; Rho, M. C.; Hayashi, M.; Komiyama, K. *Bioorg. Med. Chem. Lett.* **1998**, *8*, 2769.
- Kam, T. S.; Tan, P. S. *Phytochemistry* **1990**, *29*, 2321.
- Kam, T. S.; Lim, K. H.; Yoganathan, K.; Hayashi, M.; Komiyama, K. *Tetrahedron* **2004**, *60*, 10739.
- Kam, T. S.; Sim, K. M.; Koyano, T.; Toyoshima, M.; Hayashi, M.; Komiyama, K. *J. Nat. Prod.* **1998**, *61*, 1332.